INTERNATIONAL JOURNAL FOR NUMERICAL AND ANALYTICAL METHODS IN GEOMECHANICS, VOL. 20, 693–713 (1996)

BOUNDARY LAYER TRANSPORT OF METAL IONS IN FROZEN SOIL

A. M. O. MOHAMED*, I. SHOOSHPASHA† AND R. N. YONG‡

Geotechnical Research Centre, McGill University, 817 Sherbrooke St. West, Montreal, Quebec, Canada H3A 2K6

SUMMARY

Two series of freezing column tests with distilled water and municipal solid waste leachate were investigated, using illitic silty clay. Temperature distributions along the freezing column were recorded as a function of distance and time. Unfrozen moisture content and osmotic pressures as a function of temperature were calculated.

It was shown that temperature distributions as a function of distance and time were similar in all tests, probably as a result of the limited amount of moisture intake. The amount of moisture intake was directly related to freezing time and temperature gradient in the freezing column. Unfrozen moisture contents, ion concentrations and temperature gradients were identified as the controlling parameters that contributed to the boundary layer transport (BLT) of metal ions in frozen specimens. Na^+ concentration profiles were mostly dependent on water movement in the freezing column. The behaviour of Ca^{2+} and Mg^{2+} cations was similar to Na^+; their concentrations in the soil solution decreased with freezing time due to ion exchange.

Temperature, moisture content in an unfrozen boundary layer (UBL), and concentration gradient were taken into consideration in the development of a boundary layer transport model (BLTM). Based on the experimental results and Powell's optimization technique, the diffusivity parameters of various metal ions were calculated. Comparison of experimental and predicted results indicated that the BLTM can predict the migration of metal ions in UBL.

KEY WORDS: unfrozen layer; osmotic; diffusion; transport; moisture; temperature; optimization

INTRODUCTION

Two unique characteristics of the Arctic environment are permafrost and sea ice. Arctic sea ice varies seasonally from about 15 million square kilometres in winter to eight million square kilometres in sumer. The difference is equivalent in area to all the Canadian provinces combined. About half of the terrestrial area in northern Canada (10·8 million square kilometers) is underlain by permafrost ranging from less than one meter in the discontinuous layer to several tens of meters in the continuous layer.

The extent to which the permafrost will be affected by temperature is governed by the vegetation cover, properties of the soil, and the snow cover.[1] The physical and mechanical

*Associate Director, Geotechnical Research Centre, Adjunct Professor, Civil Engneering and Applied Mechanics, McGill University
†Graduate Research Assistant, Department of Civil Engineering and Applied Mechanics, McGill University
‡William Scott Professor, Department of Civil Engineering and Applied Mechanics, McGill University

CCC 0363–9061/96/100693–21

Received 17 March 1995
Revised 11 December 1995

properties of permafrost are temperature-dependent, and the creep properties of the frozen soil and ice are greatly affected by temperature changes in the permafrost, especially when the permafrost temperature is within 1 or 2°C of freezing.[2] During the transition period from discontinuous to permafrost free regions, and from continuous to discontinuous regions, considerable instability will occur in the terrestrial environment. Frost heave, contaminant migration in the unfrozen boundar layer, substantial settlement, development of thermokarst lakes, massive slope detachments and landslides in hilly areas are all expected to occur.[3]

Buried waste and pipelines laid in the permafrost areas of the north are very susceptible to any changes in the temperature of the permafrost. Soluble metal ions can move in the boundary layer under freezing conditions.[4, 5] Frost heave can cause rupture to the pipelines which in turn result in contamination of the surrounding environment. Contamination can include leakage of oil to waterways, impacting adversely on vegetation, plants, fish, birds and eventually human, who may consume any of the above as food or who may drink the contaminated water. Spillage of oil resulting from ruptures of pipes have a serious impact on the socio-economic wellbeing of the surrounding areas.

The analysis of the effect of a thermal gradient on the combined transfer of heat, moisture and solutes in soil is a complex problem with various interacting variables. Moisture transfer may occur in the liquid and vapour phases and possibly in the ice phase, due to the temperature differences, owing to movement of pore ice.[6] Heat conduction is complicated by the changing thermal conductivities that are produced by water transfer.[7] Liquid moisture carries thermal energy directly, although this is negligible compared with the heat transferred by thermal conduction through the soil.[6] The magnitude of the temperature influences the ice, liquid and vapour phase and the condition of the water in soil and the interaction of water with the internal soil surfaces. Variations in temperature lead to changes in the equilibrium between water phases, or accentuate the disequilibrium, and create water movement.[8]

The transfer of heat and moisture in frozen soils has been investigated by various researchers.[5,8-11] It has been demonstrated that in an unfrozen boundary layer (UBL) moisture is mobile at temperature as low as − 14°F and forms a continuous channel measuring up to 25 Å, through which ions could be mobile.[5] The thickness of UBL depends mainly on soil type, specific surface area, temperature, and the amount and type of dissolved solids. The diffusion of contaminants through UBL in frozen clay barriers has received little attention.

This study is designed to experimentally evaluate the effect of freezing on the redistribution of moisture and ion concentrations in unsaturated illitic silty clay soil. Soil samples were compacted at the optimum water content and maximum dry density using distilled water and then subjected to different freezing conditions. The water intake during the freezing tests was introduced in two ways, using distilled water at *p*H 5·8 as a control, and using municipal waste leachate at *p*H 6·9. After each freezing test, moisture redistribution and ion concentration in soil pore fluid were evaluated. A boundary layer transport model (BLTM) was developed taking into consideration temperature, volumetric moisture content (VMC) and concentration gradients in UBL. By using the experimental data and Powell's optimization technique, the diffusivity parameters of various metal ions were calculated and used to predict the movement of metal ions in UBL under freezing conditions.

MATERIALS AND METHODS

Soil material

The illitic silty clay soil used in this study was air dried and ground to pass through a 2 mm sieve. The dried material was then subjected to physical and chemical tests as shown in Table I.

Table I. Selected properties and compositions of illitic silty clay soil

Geotechnical properties		*Chemical properties*	
Consistency limit			
Liquid limit (%)	33·5	Soil *p*H	8·4
Plastic limit (%)	20·8	(1:10 soil:water)	
Plasticity index (%)	12·5	Cation-exchange capacity	
		Na, K (cmol/kg)	40
		Ca, Mg (cmol/kg)	20
Compaction			
Maximum dry density (Mg/m^3)	1·84	Surface area ($m^2/kg \times 10^{-3}$)	92
Optimum moisture content (%)	16·5	Total organic content (% w/w)	0·9
		Carbonate content (% w/w)	14·7
Grain size analysis		Amorphous content	
D_{50} (μm)	5·0	S_iO_2	2·1
D_{10} (μm)	0·4	Fe_2O_3	3·6
C_u	20·3	Al_2O_3	1·1
Cc	3·1	Total	6·8

Mineralogical composition (given in a decreasing order) illite, chlorite, quartz, feldspar, calcite

Soil *p*H was measured in 1:10 soil:water solution ratio by a Beckman I™ 12 *p*H/ISE meter. Cation exchange capacity was determined at *p*H 7 using the silver thiourea method.[12] The surface area was measured using ethylene glycomono-ethylether (EGME), according to the procedure described by Eltantaway and Arnold;[13] the total organic content was determined following the method described by Jackson;[14] the carbonate content determination was carried out using the titration method;[15] the presence of amorphous materials was determined using the Segalen technique,[16] and the percentage of clay was determined by the particle size analysis method in accordance with ASTM, D698-78.[17]

Leachate solution

The soil uptake solutions, during the freezing process, were (i) distilled water as a control, *p*H = 5·8, and (ii) municipal solid waste leachate collected from a landfill in Montreal. The leachate was collected directly from a leachate-collector tank, then stored in a freezer to prevent possible changes in chemical composition (see Table II for leachate characteristics). This case was chosen to simulate the performance of a clay barrier under neutral conditions and to study the effect of ion competition in a multi-component system of leachate.

Soil preparation

Prior to freezing the dry soil was mixed with distilled water at the optimum water content. The soil was then placed in a plastic container and allowed to equilibrate in a humid room for at least 24 h and then compacted in a lucite cell to its maximum dry density in eleven equal layers of 10 mm. The weight of soil needed for the inidividual compacted layers was calculated from the maximum dry density and initial moulding water content, which was generally 1 per cent higher than the optimum water content.

Table II. Ion concentration in leachates

Parameter	Concentration (mg/l) Municipal landfill leachate
*p*H	6·9
Redox potential (mV)	112
Cations	
Na^+	1165
K^+	325
Ca^{2+}	92
Mg^{2+}	165
Anions	
NH^4	192
Cl^-	1515
SO_4^{2-}	27
Heavy metals	
Pb^{2+}	< 0·1
Cu^{2+}	< 0·1
Zn^{2+}	0·2
Cd^{2+}	< 0·1

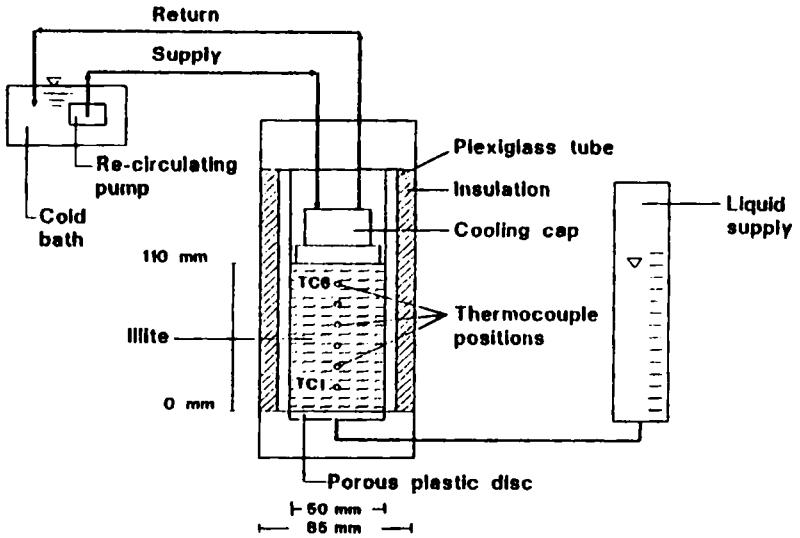

Figure 1. Schematic diagram of the test apparatus

Test apparatus

A schematic diagram of the test apparatus is shown in Figure 1. The soil samples were subjected to freezing procedures in four lucite cells. Each cell consisted of a cylinder measuring 200 mm in height and 50 mm in internal diameter, a base with a port for fluid supply, and a ring at the top of the cylinder. To prevent leaks, a rubber O-ring was placed between the bottom of the

Table III. Initial and boundary conditions of various experiments

Series no.	Test no.	Initial water content (%)	Pressure head (mm)	Water (ml) intake	Onset time of freezing (h)	Av. temp. (°C)		Temperature gradient (°C/cm)		Duration of test (h)
						bottom	top	Frost front	In frozen soil	
First	1	17·2	131	3·4	13·0	− 1·6	− 7·2	0·88	0·51	24
distilled	2	16·6	147	3·4	12·0	− 3·5	− 9·3	0·68	0·61	47·5
water	3	17·9	135	4·4	16·0	− 1·35	− 8·3	1·26	0·56	99·5
	4	17·6	131	6·0	21·5	− 0·8	− 7·2	1·13	0·54	191
	5	17.9	134	4·0	18·0	− 2·05	− 8·1	1·09	0·50	384
Second	6	17·9	147	5·0	10·5	− 2·3	− 8·3	1·09	0·54	22·5
municipal	7	17·5	145	6·8	10·0	− 3·9	− 13	1·29	0·79	48
leachate	8	17·3	164	4·0	9·0	− 3·7	− 12	1·45	0·78	96
	9	17·3	138	5·8	10·5	− 3·5	− 13	1·31	0·84	192
	10	16·6	140	5·4	11·5	− 2·5	− 9·8	0·83	0·68	384

cylinder and the base of the cell. During the experiment fluid was supplied by means of nylon tubing connected to the bottom of a burette containing water or leachate and attached to the base of each cell. To check for temperature changes, six thermocouples were installed at equal intervals between top and bottom of the freezing column (Figure 1) The cooling cap, connected to a cold bath was placed on top of the soil sample.

Experimental procedures

After compacting the soil in the cylinder, thermocouples were inserted into the soil column. The cell was then wrapped with plastic seal and two layers of fibre-glass insulation. The burette, filled with selected leachate, was attached by tubing to the bottom of the cylinder and the cell was connected to the cooling system. The specimens were allowed access to the fluid uptake from the beginning to end of each test. The pressure heads at the base of the specimens and the resultant hydraulic gradients are shown in Table III. The temperatures of the cold bath and the cooling cap for different experiments varied from $-16°C$ to $-19.5°C$ and from $-11°C$ to $-14.5°C$, respectively. The temperature of the cold room where the tests were performed ranged from 2.8°C to 4.5°C.

Depending upon the type of intake fluid, two test series, composed of five experiments each with time durations of 1, 2, 4, 8, and 16 days, were conducted. After freezing for the specified length of time, each sample in its frozen state was removed from the cell, then cut into eleven sections for moisture content determination and chemical analysis of the pore fluid.

The initial and boundary conditions for all the tests for Series 1 and 2 are listed in Table III. The amount of moisture uptake increases with the increased period of freezing, which indicates that the system is open during freezing.

RESULTS AND DISCUSSIONS

Temperature distribution

The temperature distributions, for tests 1–10, as a function of distance and time were similar despite various test durations and type of uptake fluids. Therefore, as an example, temperature distribution profiles over a 24 h period for test 1 are shown in Figure 2. For the most part, temperature within the soil specimens decreased from the initial temperature (i.e. room temperature) to a specified temperature, which is controlled by the cooling system as a function of time. Within the first three hours, temperature distributions are highly non-linear. For a longer period of freezing, temperature distributions are stabilized and reach steady state conditions after 13 h. For time periods greater than 24 h, the temperature distribution reaches a steady-state condition and continues at that state to the end of each test.

Moisture redistribution

During freezing, soil pore fluid exists in both frozen and unfrozen states. To determine the quantities of unfrozon moisture contents (UMC), the DSC test chamber is used.[5] Typical calculated values of UMC for distilled water are shown in Figure 3 depicting the relationships between fluid content, distance from fluid source intake during freezing, and temperature. As temperature is decreased, UMC is decreased and the total pore fluid increases, which is attributed

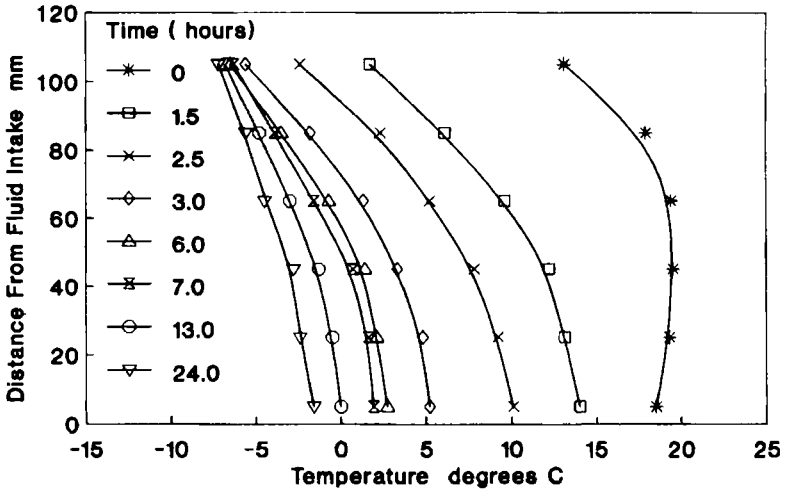

Figure 2. Temperature distribution profiles for test 1 in series 1

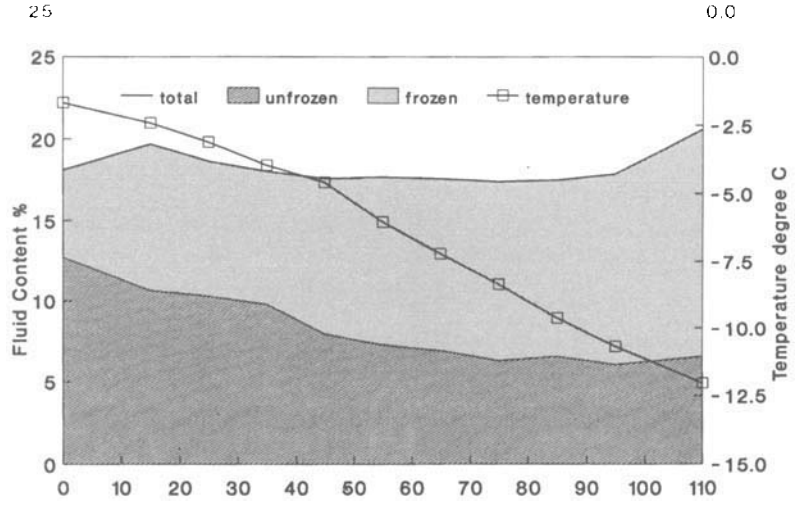

Figure 3. Speciation of soil pore fluid during freezing for soil and distilled water

to ice formation and moisture migration to lower temperatures zones. As distance from fluid intake is increased, UMC is decreased in accordance with the temperature changes. The small differences in total moisture content (up to 1 per cent) occurring as a result of moisture migration through the frozen soil does not seem to influence the UMC at a given temperature. This in turn suggests that UMC does not change once the temperature distribution reaches steady state condition. Differences in UMC between soil frozen with distilled water and with leachate are slight and conditioned mainly by temperature. It was noted that the chemistry of the intake fluid did not influence the UMC, probably because the amount of the fluid taken by the soil during freezing was low.

UMC–temperature relationship

The variations of UMC with temperature for both distilled water and leachate solutions are combined and replotted as shown in Figure 4(a). The functional relationship between UMC and temperature is also shown in Figure 4(a). The relationship is best described by the following Gaussian equation:

$$W_{uf} = 5{\cdot}66 + 30{\cdot}19 \exp\left[-0{\cdot}5 \left(\frac{T - 110{\cdot}02}{-6{\cdot}77} \right)^2 \right] \quad (1)$$

where W_{uf} is UMC in percentage; T is the temperature in degrees Celsius.

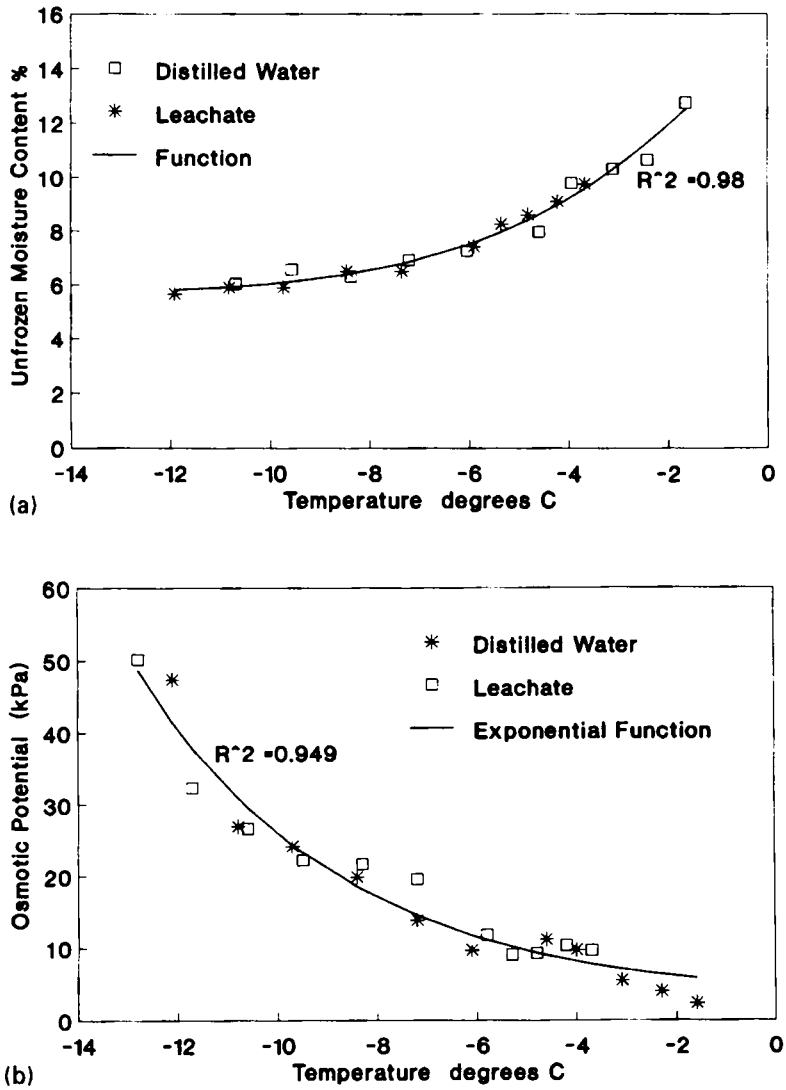

Figure 4(a). Variations of unfrozen moisture content with temperature. (b) Osmotic potential and temperature relationship

Osmotic potential–temperature relationships

To calculate the resultant osmotic potential due to the increase in cation concentration one adopts a similar technique to that reported by Yong *et al.*[11] During freezing, moisture moves from the internal mineral layers out into the surrounding pores to join an ice crystal. This causes a decrease in the spacing between mineral layers and an increase in osmotic pressure. As the temperature is reduced, more moisture moves to the ice crystal and osmotic pressure increases. The partial molar free energy of soil water, $(\bar{F}_w - \bar{F}_w^0)$, can be related to the osmotic potential, by the following relationship:[18]

$$\bar{F}_w - \bar{F}_w^0 = -V_w \psi_\pi \tag{2}$$

where $\bar{F}_w$ is the molar free energy at any state, $\bar{F}_w^0$ the molar free energy at a reference state; V_w the partial molar volume of the water in soil, and ψ_π the osmotic potential. The difference in partial molar volume can also be obtained as[18]

$$\bar{F}_w - \bar{F}_w^0 = RT \ln a_1 \tag{3}$$

where R is the gas constant; T the absolute temperature, and a_1 the activity of soil water. When a soil pore fluid is subjected to freezing, the free energy of solid water (ice) at equilibrium state is assumed[11] to be equal to the partial molar free energy of soil water adjacent to the soil particle surface:

$$\bar{F}_s^0 = \bar{F}_w \tag{4}$$

where the subscripts s and w denote soil and water states. Since, the partial free energy of soil water is given by

$$\bar{F}_w = F_w^0 + RT \ln a_1 \tag{5}$$

by substitution and differentiation, one obtains

$$\frac{d}{dT}(\ln a_1) = -\frac{1}{R}\frac{d}{dT}\left(\frac{\Delta \bar{F}_{fusion}^0}{T}\right) \tag{6}$$

The second term in the right-hand side of (6) is further expressed by Yong *et al.*[11] as follows:

$$\frac{d}{dT}\left(\frac{\Delta \bar{F}_{fusion}^0}{T}\right) = -\frac{\Delta \bar{H}_{fusion}^0}{T^2} \tag{7}$$

Substituting equation (7) into (6), one obtains

$$\frac{d}{dT}(\ln a_1) = -\frac{\Delta \bar{H}_{fusion}^0}{RT^2} \tag{8}$$

If one further assumes that $\Delta \bar{H}_{fusion}^0$ is a piecewise constant over a small temperature change from T_f to T_f', where T_f is freezing temperature of ice (273°C) and T_f' is the freezing temperature of the system that is less than T_f. By integrating equation (8) from pure solvent (T_f and a_1 not equal to 1) to soil-water solution (T_f, $a_1 = 1$), the following equation can be obtained:

$$\ln a_1 = \frac{\Delta \bar{H}_{fusion}^0}{R}\left(\frac{T_f' - T_f}{T_f T_f'}\right) \tag{9}$$

At a specified freezing temperature T_f' equation (2) can be written as

$$\bar{F}_w - \bar{F}_w^0 = RT_f' \ln a_1 \tag{10}$$

Substituting (10) into (9), one obtains

$$\bar{F}_w - \bar{F}_w^0 = \Delta\bar{H}_f^0 \left(\frac{T_f' - T_f}{T_f}\right) \tag{11}$$

By substituting (11) into (2), the osmotic potential can be expressed as follows:

$$\psi_\pi = -\frac{\Delta\bar{H}_f^0}{V_w}\left(\frac{T_f' - T_f}{T_f}\right) \tag{12}$$

The heat of fusion $\Delta\bar{H}_f^0$ and unfrozen water content necessary for calculations were found experimentally from the DSC technique. Based on (12) and the experimentally obtained results from the DSC technique, the calculated osmotic potentials for the frozen illitic silty clay soil for both distilled water and leachate solutions are shown in Fig. 4(b). In both cases, the osmotic potential increases significantly with decreasing temperature due to increasing cation concentrations in the unfrozen moisture.

The difference between the calculated osmotic potential in illitic silty clay soil frozen with distilled water and with leachate is not significant. At high temperature range, the osmotic potential is slightly higher for leachate than for water due to high cation concentrations. For a specified temperature, as distance from fluid intake is increased, the osmotic potential is at first equal, then higher for the first specimen (frozen with distilled water). This rapid increase in osmotic potential at lower temperatures is probably the effect of the highier cation concentrations. This was due to the different freezing conditions, higher temperature gradient, and longer freezing time.

For both distilled water and leachate, the experimental data, i.e., the calculated osmotic potentials based on (12) and DSC technique, are fitted with the following exponentional functions:

$$\psi_\pi = 2{\cdot}79 + 2{\cdot}03 \exp\left[-\frac{T}{4{\cdot}11}\right] \tag{13}$$

where ψ_π is the osmotic potential (kPa).

The dependence of the unfrozen moisture content and the osmotic potential on system temperature as represented by (1) and (13) will be used in the development of a BLTM.

Cations migration

Due to low hydraulic gradients across the specimens and low fluid intake during testing (as shown in Table III), it is reasonable to assume that transport of cations by advection mechanism (i.e. velocity driven due to induced hydraulic gradient) may not play a major part. Hence, the two basic phenomena that control ion redistribution in UBL are (i) transport by the unfrozen water due to temperature, and (ii) diffusion due to concentration gradient. Therefore, it is necessary to present the concentration profiles of various cations with respect to the amount of unfrozen moisture in the BL. To proceed, the calculated equilibrium concentrations of various cations were multiplied by the ratio between the total (frozen and unfrozen) moisture content over UMC. The migration profiles of Na^+, K^+, Ca^{2+} and Mg^{2+} are plotted as a function of distance from the source of fluid intake during freezing as shown in Figures 5(a)–(d) for tests performed with distilled water.

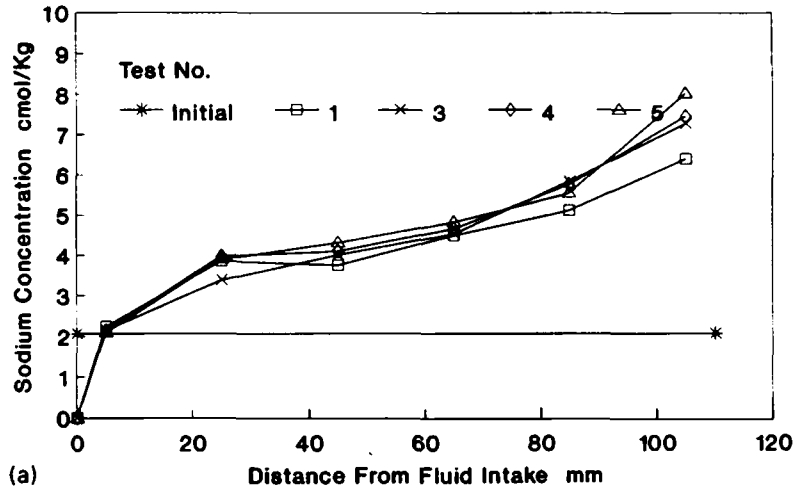

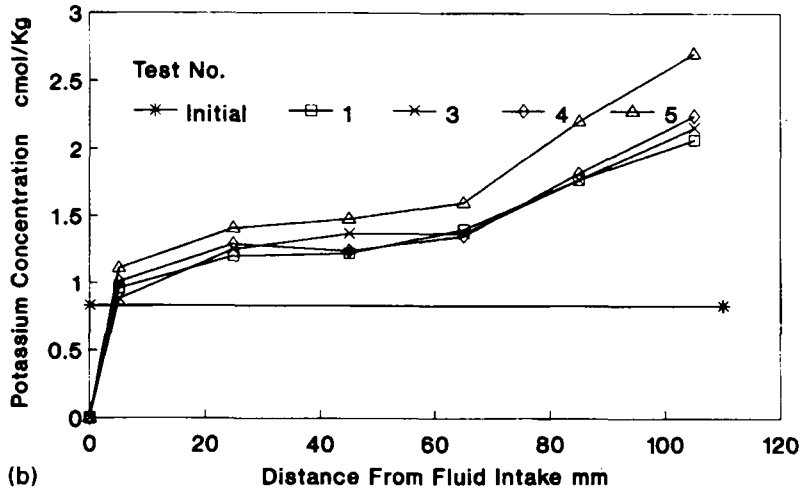

Figure 5. Continued

The redistribution of monovalent cations, Na^+ and K^+, are similar. The Na^+ concentrations in UMC in BL close to the fluid intake source are close to the initial Na^+ concentration in the total pore fluid (2·06 cmol/L). The amount of UMC in BL is very high (Fig. 3(a)). The chemical analysis of distilled water, taken from a burette after five hours of freezing, showed that the concentration of monovalent cations reached 0·0049 and 0·0028 cmol/L for Na^+, and K^+, respectively. The appearance of cations in the burette indicated that a certain amount of ions diffused downward due to concentration gradient.

As distance from fluid intake is increased, UMC is decreased, as shown in Fig. 3(a), and the concentrations of Na^+ and K^+ are increased gradually, reaching the maximum in direct contact with the cooling cap, i.e. at 110 mm distance from fluid intake. For longer periods of freezing, concentrations of monovalent cations have increased progressively for the particular time, from one to 16 days, due to ion migration. The increase in concentrations is most pronounced because

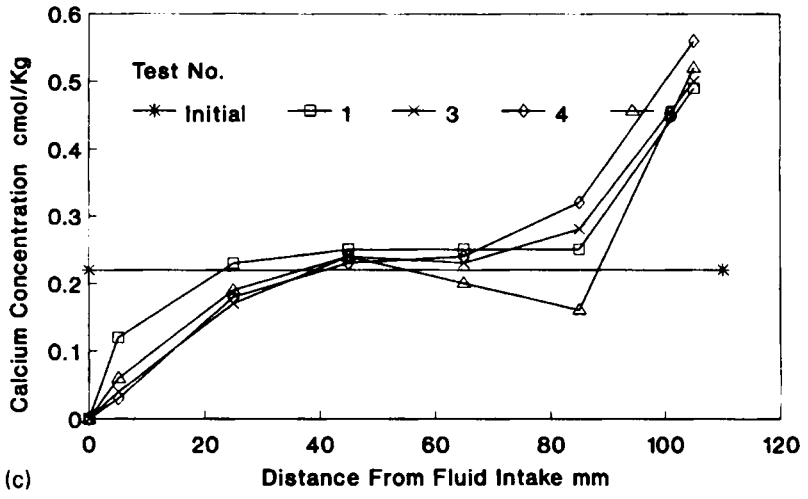

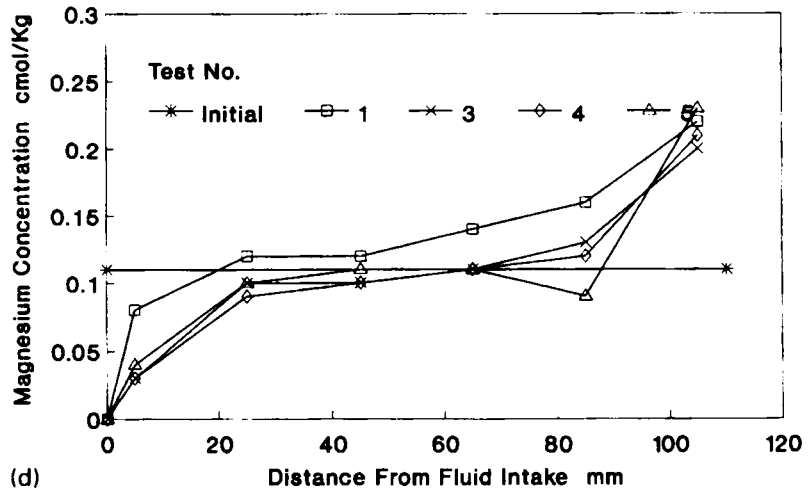

Figure 5. Migration profiles in the unfrozen water layer for series 1 for (a) sodium, (b) potassium, (c) calcium, and (d) magnesium

of the effect of low temperature. The continuous moisture and cation movements toward the top of the soil columns are attributed to both temperature and osmotic potential gradients. As time is increased, K^+ concentrations are increased. At 5 mm distance from fluid intake in tests 1, 3, 4 and 5, K^+ concentrations are higher than initial concentrations (Figure 5(b)) while, Na^+ concentrations are the same as the initial concentrations (Figure 5(a)). This is attributed to high mobility of Na^+ than K^+ ions, i.e., higher diffusion, as will be discussed.

Both divalent cations, Ca^{2+} and Mg^{2+}, show similar behaviour in the frozen soil as shown in Figure 5(c) and 5(d). In the bottom of the frozen column, between 0 and 40 mm from the source of fluid intake, the concentrations of Ca^{2+} and Mg^{2+} remained lower than their initial values,

regarding total water in pore fluid, and decreased progressively with time. The reduction of divalent cation content may be due to

(i) exchange reactions between the monovalent and divalent cations,
(ii) water and cation transfer upward to the cold soil surface, and
(iii) cation diffusion under the influence of existing concentration gradient between the soil pore solution and the distilled water in the burette.

After five hours of freezing, the cation concentrations in the distilled water increased to 0·0021 cmol/l for Ca^{2+}, and 0·00029 cmol/l for Mg^{2+}. It should be noted that the recorded concentrations of monovalent cations in the burette were higher than the divalent cations due to cation exchange.

As distance from fluid intake is increased, divalent cation concentrations are increased having higher values than initial concentrations. The increase in concentrations of Ca^{2+} and Mg^{2+} could be attributed to (i) a decrease in UMC due to temperature decrease, and (ii) an increase in moisture and cation migration due to the increase in osmotic potential gradient.

Mass balance calculations were performed to support the hypothesis of cation exchange reactions between divalent and monovalent cations. The different elements considered in the mass balance calculations, for test series 1, were (i) the total retained ions were determined from the area bounded by the initial and test five concentration profiles, and (ii) the amount of adsorbed ions was established from the relationship between sorbed and soluble ions. Since deionized water was used, the total equilibrium concentrations of various cations before and after testing should be equal. As an example, for test 5, the calculated equilibrium concentrations before and after testing were 0·437 and 0·449 cmol, respectively. The difference in percentage between the two conditions is 2.75 per cent, which is within the acceptable error in experimental measurements. A similar range of error was obtained for the other set of results.

The redistribution of cations for the second series, which included tests 6–9, resembles those for the first series. However, the cation concentrations (monovalent as well as divalent) in UBL are higher than those for tests 1–5. The concentrations of monovalent cations surpass the initial values for the soil solution due to ionic diffusion from the input leachate to the soil.

ANALYSIS OF THE EXPERIMENTAL DATA

BLTM development

The experimental results have shown that metal ions are transported through UBL due to the development of osmotic and UMC gradients. Flow of metal ions due to diffusion in one-dimension takes the following form:

$$J_c = -D_\pi \frac{\partial}{\partial x}(\theta c) \tag{14}$$

where D_π is the diffusivity parameter, $D_\pi = D_0 f(c)$; D_0 is the self-diffusion coefficient; $f(c)$ is a functional relationship whose terms depend on concentrations; θ is the volumetric moisture content (VMC) in UBL, c the solute concentration in UBL, and x the distance from the source of fluid intake.

The mass balance equation is given by

$$\frac{\partial}{\partial t}(\theta c) = -\frac{\partial J_c}{\partial x} \tag{15}$$

where t is time.

Combining (14) and (15) one obtains:

$$\frac{\partial}{\partial t}(\theta c) = \frac{\partial}{\partial x}\left(D_\pi \theta \frac{\partial c}{\partial x} + D_\pi c \frac{\partial \theta}{\partial x}\right) \tag{16}$$

Equation (16) describes metal ion transport in UBL. The experimental data have shown that θ and ψ are functions of temperature, as represented by (1) and (13). Hence, (16) can be expanded to include the effect of temperature as follows:

$$\frac{\partial}{\partial t}(\theta c) = \frac{\partial}{\partial x}\left(D_\pi \theta \frac{\partial c}{\partial T}\frac{\partial T}{\partial x} + D_\pi c \frac{\partial \theta}{\partial T}\frac{\partial T}{\partial x}\right) \tag{17}$$

Equation (17) describes metal ion transport in UBL due to subfreezing temperature gradient. Additionally, the experimental results have shown that

(i) temperature distribution along the soil column reaches a steady state in a short period;
(ii) there is a dependence of θ on T;
(iii) for a given T, moisture migration does not influence UMC, and
(vi) from DSC results, equilibrium time for heat of fusion from ice to water is 10 min.[5]

Therefore, one can assume that θ is independent of time. Hence, (17) can be reduced to:

$$\theta \frac{\partial c}{\partial t} = \frac{\partial D_\pi}{\partial c}\frac{\partial c}{\partial x}\theta \frac{\partial c}{\partial T}\frac{\partial T}{\partial x} + D_\pi \frac{\partial \theta}{\partial x}\frac{\partial c}{\partial T}\frac{\partial T}{\partial x} + D_\pi \theta \frac{\partial^2 c}{\partial T \partial x}\frac{\partial T}{\partial x} + D_\pi \theta \frac{\partial c}{\partial T}\frac{\partial^2 T}{\partial x^2}$$
$$+ \frac{\partial D_\pi}{\partial c}\frac{\partial c}{\partial x} c \frac{\partial \theta}{\partial T}\frac{\partial T}{\partial x} + D_\pi \frac{\partial c}{\partial x}\frac{\partial \theta}{\partial T}\frac{\partial T}{\partial x} + D_\pi c \frac{\partial^2 \theta}{\partial T \partial x}\frac{\partial T}{\partial x} + D_\pi c \frac{\partial \theta}{\partial T}\frac{\partial^2 T}{\partial x^2} \tag{18}$$

Furthermore, the dependence of the diffusivity parameter, D_π, on solute concentration, c, can be expressed by the following exponential function:[19,20]

$$D_\pi = a \exp(bc) \tag{19}$$

where $a(\mathrm{l}^2\,\mathrm{t}^{-1})$ and $b(\mathrm{mm}^{-1})$ are material parameters to be determined by an optimization technique and the explicit finite difference method.

Substituting (19) into (18), the following equation is obtained:

$$\theta \frac{\partial c}{\partial t} = ab\mathrm{e}^{bc}\frac{\partial c}{\partial x}\theta \frac{\partial c}{\partial T}\frac{\partial T}{\partial x} + a\mathrm{e}^{bc}\frac{\partial \theta}{\partial x}\frac{\partial c}{\partial T}\frac{\partial T}{\partial x} + a\mathrm{e}^{bc}\theta \frac{\partial^2 c}{\partial T \partial x}\frac{\partial T}{\partial x} + a\mathrm{e}^{bc}\theta \frac{\partial c}{\partial T}\frac{\partial^2 T}{\partial x^2}$$
$$+ ab\mathrm{e}^{bc}\frac{\partial c}{\partial x} c \frac{\partial \theta}{\partial T}\frac{\partial T}{\partial x} + a\mathrm{e}^{bc}\frac{\partial c}{\partial x}\frac{\partial \theta}{\partial T}\frac{\partial T}{\partial x} + a\mathrm{e}^{bc}c \frac{\partial^2 \theta}{\partial T \partial x}\frac{\partial T}{\partial x} + a\mathrm{e}^{bc}c \frac{\partial \theta}{\partial T}\frac{\partial^2 T}{\partial x^2} \tag{20}$$

Generally, there are two approaches for solving the general partial diffusion equations either analytically or numerically. In this study, the explicit finite difference method was used to solve (20) numerically. The concentrations at time $j + 1$ are given by:

$$c_i^{j+1} = \frac{\Delta t}{4\theta_i \Delta x^2} abe^{bc_i^j}\Bigg[b\theta_i(c_{i+1}^j - c_{i-1}^j)^2 + (\theta_{i+1} - \theta_{i-1})(c_{i+1}^j - c_{i-1}^j) + 4\theta_i(c_{i+1}^j - 2c_i^j + c_{i-1}^j) + 4\theta_i \frac{c_{i+1}^j - c_{i-1}^j}{T_{i+1} - T_{i-1}}(T_{i+1} - 2T_i + T_{i-1}) + bc_i^j(c_{i+1}^j - c_{i-1}^j)(\theta_{i+1} - \theta_{i-1}) + (c_{i+1}^j - c_{i-1}^j)(\theta_{i+1} - \theta_{i-1}) + 4c_i^j(\theta_{i+1} - 2\theta_i + \theta_{i-1}) + 4c_i^j \frac{\theta_{i+1} - \theta_{i-1}}{T_{i+1} - T_{i-1}}(T_{i+1} - 2T_i + T_{i-1})\Bigg] + c_i^j \tag{21}$$

Determination of diffusivity parameter

As indicated by (21), if the diffusivity parameter and concentration profile at time j are known, the concentration profile at time $j + 1$ can be found numerically. Thus, by having an experimentally measured concentration profile at a certain time and an assumed function for the diffusion parameter, one can predict the concentration profile at the next time step. The next time step is the time at which the concentration profile is experimentally measured. The optimization procedure relied on the use of the following function to obtain the optimum diffusion parameters (i.e. a and b).

$$F = \sum_{i=1}^{N} |c_{\text{exp}} - c_{\text{calc}}| \tag{22}$$

where N is the number of points at which the unfrozen volumetric moisture contents were measured, c_{exp} the experimentally obtained concentrations in the unfrozen moisture and c_{cal} is the calculated concentrations in UBL by the finite difference technique.

Thus, for each chosen diffusivity parameters, F can be calculated. It is not evident how F behaves since the chosen diffusion parameters may vary. Therefore, the best way to obtain a minimum value of F is to use a search technique. One of the most efficient search techniques is Powell's conjugate directions method of non-linear optimization.[21] For the problem under consideration, the derivative of F with respect to a specific unknown parameter, cannot be simply determined. Powell's method is thus more useful because it does not require derivatives of the objective function.

BLTM calibration

To calibrate the BLTM, experimental results of each test series were used to determine the unknown parameters a and b of equation (19). To achieve this goal, the finite difference solution technique was combined with Powell's optimization technique as shown in Figure 6. In the solution technique the correlation coefficient r, which indicates the relationship between measured and calculated concentrations, is calculated by using the following equation:

$$r = \sqrt{1 - \frac{\sum_{i=1}^{n} [c_{(\text{exp } i)} - c_{(\text{calc } i)}]^2}{\sum_{i=1}^{n} [c_{(\text{exp } i)} - c_{(\text{avr})}]^2}} \tag{23}$$

where c_{avr} is an average of the measured concentrations in the unfrozen moisture.

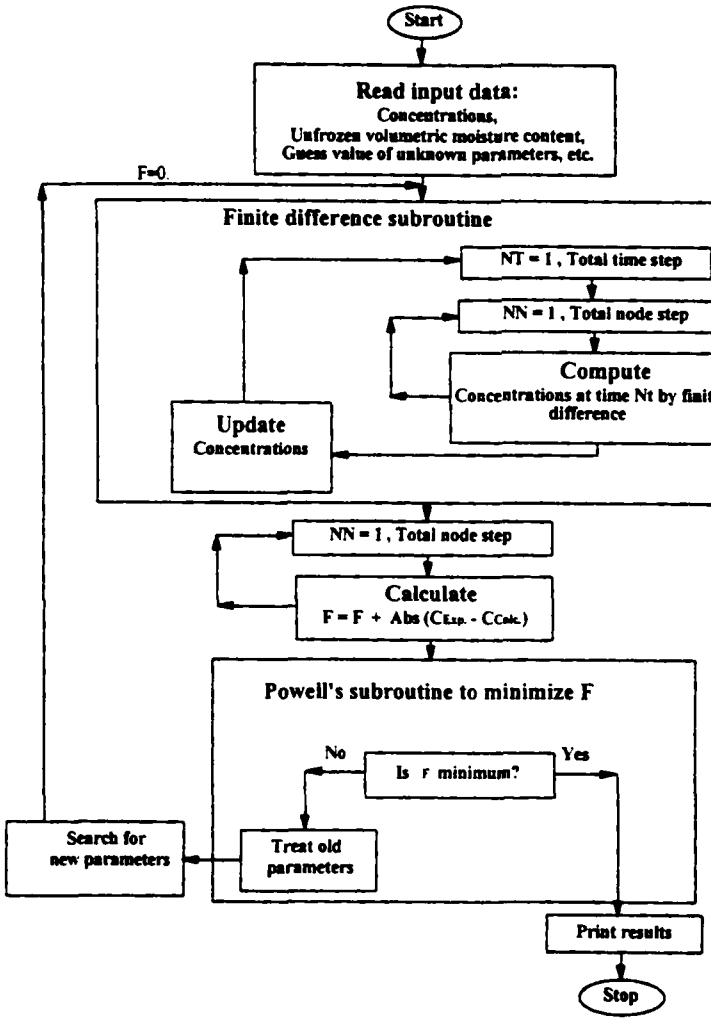

Figure 6. Calibration program flow chart

Using the aforementioned solution technique, and Tests 4 and 9 for Series 1 and 2 respectively, the unknown parameters a and b were determined as shown in Table IV. Using the given parameters in Table IV, the diffusivity parameters can be calculated. Both the experimental data and the calibrated results are shown in Figures 7(a) and 7(b) for Series 1 and 2, respectively, from which it can be seen that experimental and predicted results are in close agreement.

The calculated diffusivity parameters for Na^+, K^+, Ca^{2+}, and Mg^{2+} are shown in Figures 8(a) and 8(b) for Series 1 and 2, respectively. For each cation, the diffusivity parameter increases with concentrations and distance from fluid intake. For Series 1, the order of metal ion diffusion is $Na^+ > K^+ > Mg^{2+} > Ca^{2+}$. This can be explained in view of ion radius and valence. For larger ionic radius and lower valence, the diffusivity parameter increases.[5] For Series 2, the order of metal ion diffusion is $Ca^{2+} > Na^+ > K^+ > Mg^{2+}$. The increase in Ca^{2+} diffusivity parameter is attributed to high input leachate concentrations.

Table IV. Calculated diffusivity parameters for series 1 and 2

Test condition		Metal ions Na^+	K^+	Ca^{++}	Mg^{++}
Series 1 (Distilled water)	a (mm^2/d)	458·64	1293·23	14·16	1277·64
	b (kg/cmol)	0·21	0·10	3·71	0·94
Series 2 (municipal leachate)	a (mm^2/d)	30174·50	30160·50	203·70	7774·85
	b (kg/cmol)	6·95E − 5	6·93E − 5	5·30	2·26

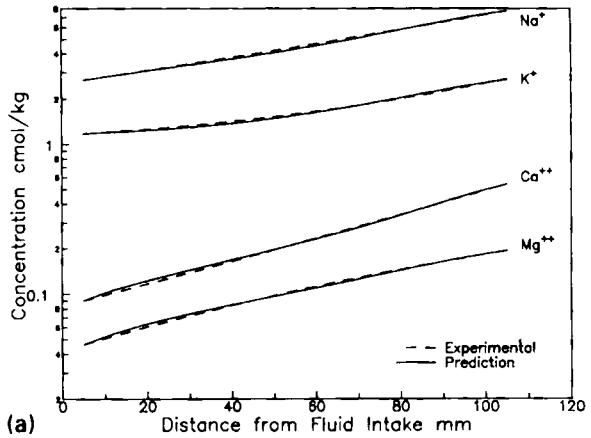

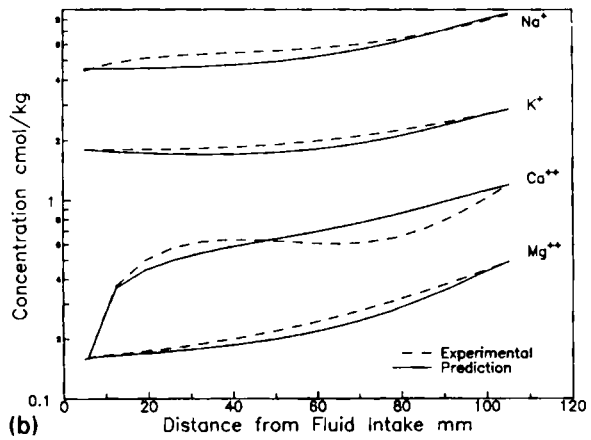

Figure 7. BLTM calibration results for (a) series 1, and (b) series 2

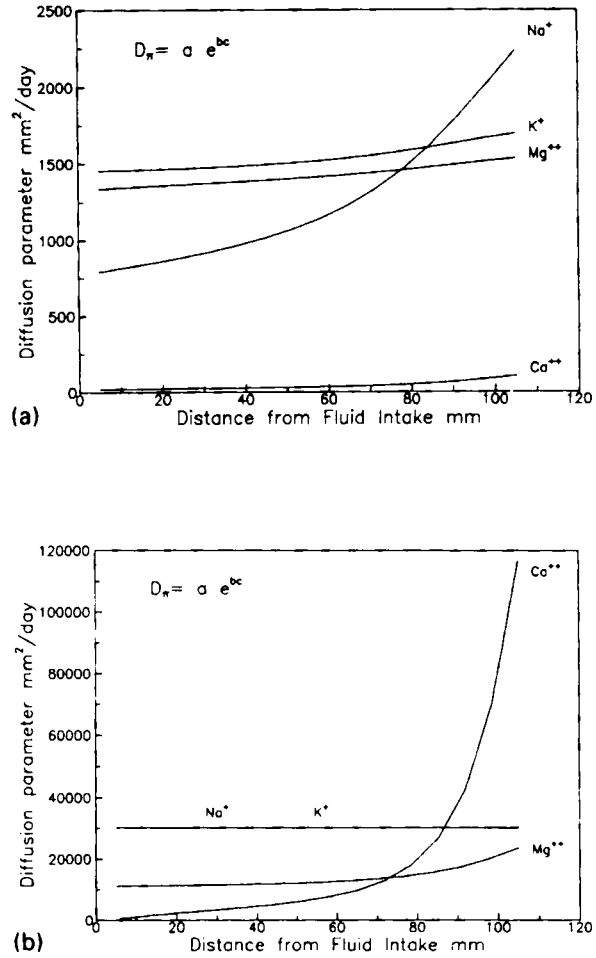

Figure 8. Variations of diffusivity parameters with distance from fluid intake for (a) series 1, and (b) series 2

BLTM prediction

With the known diffusivity parameters for each test and using equation (21), it is possible to calculate the concentration profile at any time step by the finite difference method. In this regard, a Fortran program was developed to predict concentration variations with distance. The calculated results are shown in Figures 9 and 10 for Series, 1 and 2, respectively. The predicted results simulate the experimental data for both series for distance greater than 5 mm from the source of fluid intake. The inadequacy of predicting the exact phenomena at the boundnary is attributed to the complex redistribution of metal ions as indicated by the experimental results, i.e. the opposite diffusion from the specimen to the burette due to osmosis. However, BLTM predicts metal ion movements in UBL due to temperature, UMC and concentration gradients to the satisfaction of engineers.

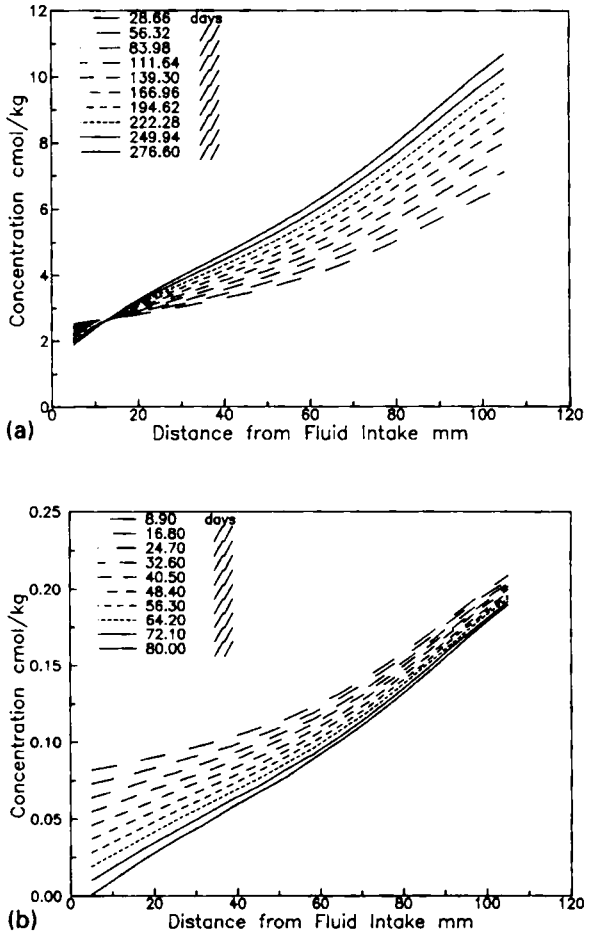

Figure 9. Predicted concentration variations with distance from fluid intake for series 1: (a) Na^+, and (b) Mg^{++}

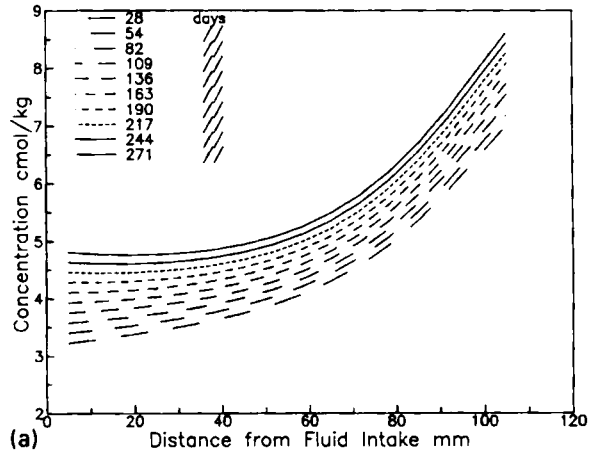

Figure 10. Continued

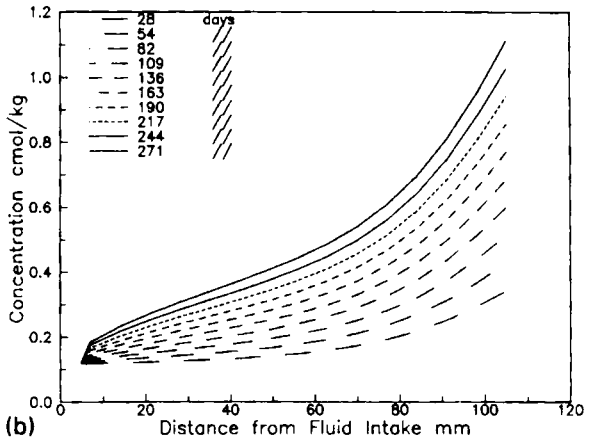

Figure 10. Predicted concentration variations with distance from fluid intake for series 2: (a) Na^+, and (b) Mg^{++}

CONCLUSIONS

The effect of freezing on the redistribution of moisture and metal ion concentrations in frozen soil was investigated experimentally. Two types of fluid intake during freezing were used. It was shown that the temperature distributions along the specimens were similar in all tests due to the limited amount of mositure intake during freezing. Also, the temperature stabilized within the specimen in 24 h. UMC and osmotic potential at steady state temperature were functions of temperature. Metal ion concentration profiles in UBL depended to a large degree on ionic diffusion. Cation distributions as a function of distance from the source of fluid intake and time were different for each specific metal ion.

BLTM was developed to predict the experimental results. Temperature, UMC and concentration gradients were taken into consideration in the model development. The diffusivity parameter for each metal ion was calculated by using the experimental results and an optimization technique. It was observed that the diffusivity parameters depended on both concentration and temperature. The BLTM will be of value in the prediction of movement of metal ions in UBL during the freezing process for the design of clay barrier systems in cold regions.

ACKNOWLEDGEMENT

This study was supported by the Natural Sciences and Engineering Research Council of Canada, Grant. No. OGP0046418 to A.M.O. Mohamed.

REFERENCES

1. M. Smith, 'Potential responses of permafrost to climatic change', *J. Cold Regions Eng.*, **4**(1), 29–37 (1990).
2. D. C. Esch and T. E. Osterkamp, 'Cold regions engineering: climatic warming concerns for Alaska', *J. Cold Regions Eng.*, **4**(1), 6 14 (1990).
3. J. Gerwick and C. Ben, 'Effect of global warming on arctic coastal and offshore engineering', *J. Cold Regions Eng.*, **4**(1), 1- 5 (1990).
4. I. K. Iskandar, 'The effect of freezing on the level of contaminants in uncontrolled hazardous waste sites', U.S. Army Corps of Engineers, Cold Regions Research & Engineering Laboratory, *Special Report* 86- 19, 1986.
5. A. M. O. Mohamed, R. N. Yong and M. Mazus, 'Contaminant migration in engineered clay barrier due to heat and moisture redistribution under freezing conditions', *Can. Geotech. J.*, **32**(1), 40–59 (1995).

6. O. T. Farouki, *Thermal Properties of Soils*, Trans. Tech. Pub., 1986.
7. R.N. Yong, P. Boonsinuk, and A.E. Tucker, 'Cyclic freeze-thaw influence on frost heaving pressures and thermal conductivities of high water content clays', *Proc. Fifth Int. Offshore Mechanics and Arctic Engineering Symp., IV, ASME*, 1986, pp. 277–284.
8. A. M. O. Mohamed, R. N. Yong and M. Mazus, 'Performance evaluation of engineered clay cover subjected to different environmental conditions', *Int. Conf. Environment and Geotechniques; from decontamination to protection of the subsoil*, Ecole Nationale des Ponts et Chaussees, Paris, 1993, pp. 571–579.
9. D. M. Anderson and A. R. Tice, 'Low temperature phases of interfacial water in clay water system', *Proc. Soil Science Society of America*, **35**, 47–54 (1971).
10. G. S. Taylor and J. N. Luthin, 'A model for coupled heat and moisture transfer during soil freezing', Can. Geotech. J., **15**, 548–555 (1978).
11. R. N. Yong, S.C.H. Cheung and D. E. Sheeran, 'Prediction of salt influence on unfrozen water content in frozen soils', *Eng. Geol.*, **31**, 137–155 (1979).
12. R. Chhabra, J. Pleysier and A. Cremers, 'The measurement of the cation exchange capacity and exchangeable cations in soil: A new method', *Proc. Int. Clay Conf.*, Applied Publishing Ltd, Illinois, 1975 pp. 439–448.
13. I. N. Eltantaway and P. W. Arnold, 'Reappraisal of ethylene glycol mono-ethylether (EGME) method for surface area estimations of clays', *Soil Sci.*, **24**, 232–238 (1973).
14. M. L. Jackson, '*Soil Chemical Analysis*', Prentice-Hall, New Delhi.
15. P. R. Hesse, 'A textbook of soil chemical analysis', William Clowes and Sons, London, 1971.
16. P. Segalan, 'Note sur une methode de determination des produits mineraux amorphes dans certains sols a hydroxides tropicaux', *Cahiers ORSTOM*, Serie, Pedologie, **6**, 105–126 (1968).
17. ASTM, 'Test methods for moisture density relations of soils and soil aggregate mixtures', (D698-78), *ASTM Annual Book of ASTM Standards*, Vol. 04.08, *Soil and Rock; Building Stones*, ASTM, Philadelphia, PA, 1984, pp. 201–207.
18. R. N. Yong and B. P. Warkentin, 'Introduction to soil behaviour', Mcmillan, New York.
19. R. N. Yong and H. M. V. Samani, 'Modelling of contaminant transport in clays via irreversible thermodynamics', ASCE-GT Specialty Conf. on Geotechnical Practice for Waste Disposal, Ann Arbor, Michigan, ASCE Geotechnical Speciality Publications, New York, 1987. Vol. 13, pp. 486–860.
20. R. N. Yong, A. M. O. Mohamed and B. P. Warkentin, 'Principles of contaminant transport in soils', Elsevier, Amsterdam, 1992.
21. M. J. D. Powell, 'An efficient method for finding the minimum of a function of several variables without calculating derivatives', *Comput. J.*, **7**, 155–162 (1964).
22. A. M. O. Mohamed, R. N. Yong, B. K. Tan, A. Farkas and L. W. Curtis, 'Geo-environmental assessment of a micaceous soil for its potential use as an engineered clay barrier, *Geotech. Testing J., GTJODJ*, **17**(3), 291–304 (1994).